JOC The Journal of Organic Chemistry

Article

pubs.acs.org/joc

Mechanistic Insights into a BINOL-Derived Phosphoric Acid-Catalyzed Asymmetric Pictet–Spengler Reaction

Lois M. Overvoorde,[†] Matthew N. Grayson,[†] Yi Luo,[§] and Jonathan M. Goodman*[,†]

[†]Centre for Molecular Informatics, Department of Chemistry, University of Cambridge, Lensfield Road, Cambridge CB2 1EW, United Kingdom

[§]Department of Chemistry, University College London, 20 Gordon Street, London WC1H 0AJ, United Kingdom

Supporting Information

ABSTRACT: The reaction of tryptamine and (2-oxocyclohexyl)acetic acid can be catalyzed by 3,3′-bis-(triphenylsilyl)-1,1′-bi-2-naphthol phosphoric acid to give an asymmetric β-carboline. This reaction was first studied by Holloway et al. (*Org. Lett.* **2010**, *12*, 4720–4723), but their mechanistic work did not explain the high stereoselectivity achieved. This study uses density functional theory and hybrid quantum mechanics/molecular mechanics calculations to investigate this reaction and provide a model to explain its outcome. The step leading to diastereo- and enantioselectivity is an asymmetric Pictet–Spengler reaction involving an *N*-acyliminium ion bound to the catalyst in a bidentate fashion. This interaction occurs via hydrogen bonds between the two terminal oxygen atoms of the catalyst phosphate group and the hydrogen atoms at N and C_2 of the substrate indole group. These bonds hold the transition structure rigidly and thus allow the catalyst triphenylsilyl groups to influence the enantioselectivity.

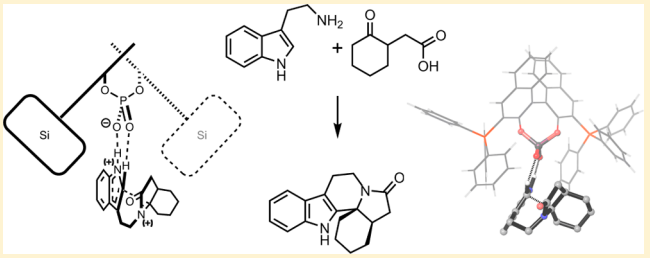

1. INTRODUCTION

This study uses computational methods to investigate the enantioselective cascade reaction shown in Scheme 1, which

Scheme 1. Reaction Studied Experimentally by Holloway et al.[1]

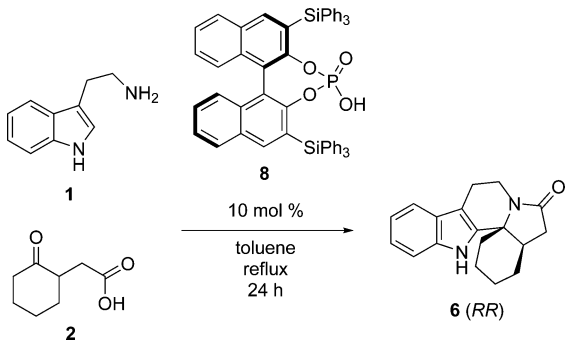

was studied experimentally by Holloway et al.[1] as part of an approach to synthesize (−)-subincanadine B.[2] The reaction involves the formation of a chiral quaternary carbon center via an asymmetric Pictet–Spengler reaction between tryptamine and (2-oxocyclohexyl)acetic acid.

The Pictet–Spengler reaction[3] was first discovered in 1911 by Amè Pictet and Theodor Spengler and has since been used in the synthesis of many natural products including (−)-suaveoline,[4] (±)-deoxyfrenolicin,[5] and (+)-coccinine.[6] It is also found in nature in the biosynthesis of many indole alkaloids, including strictosidine[7] and norcoclaurine.[8] The reaction occurs between a β-arylethylamine, such as tryptamine, and an aldehyde or ketone to form a cyclic product. There is some controversy over the reaction pathway (Scheme 2): the *N*-acyliminium ion (**3**) can either fold up via a five-membered transition structure (**TSI**) to a five-membered intermediate (**4**) followed by ring expansion (**TSIII**) to a six-membered intermediate (**5**), or it can react directly via a six-membered transition structure (**TSII**) to give the six-membered intermediate (**5**). Five-membered ring formation, as seen in **TSI**, is usually entropically favored.[9,10] Furthermore, C_3 of an indole is more nucleophilic than C_2 because reaction at C_2 disturbs the π-system of the benzene ring.[11] However, six-membered ring formation, as seen in **TSII**, could be favored due to reduced angle strain,[12] and the formation of the spiro center in **TSI** could be disfavored by steric crowding. In addition, Baldwin's rules point to the 6-*endo-trig* process being favored over the 5-*endo-trig*.[13]

Bailey et al.[14] found experimentally that formation of the five-membered intermediate in the synthesis of 3-azatetrahydro-β-carboline is fast and reversible and that formation of the six-membered intermediate is rate-determining. They could not, however, say whether the six-membered intermediate was formed directly or by ring expansion from the five-membered intermediate. When studying related Pictet–Spengler reactions computationally, Maresh et al.[7] and Kowalski et al.[15] both found that the ring-expansion transition structure (TS) was

Received: December 12, 2014
Published: February 5, 2015

DOI: 10.1021/jo5028134
J. Org. Chem. 2015, 80, 2634–2640

Scheme 2. Five- and Six-Membered Ring Pathways

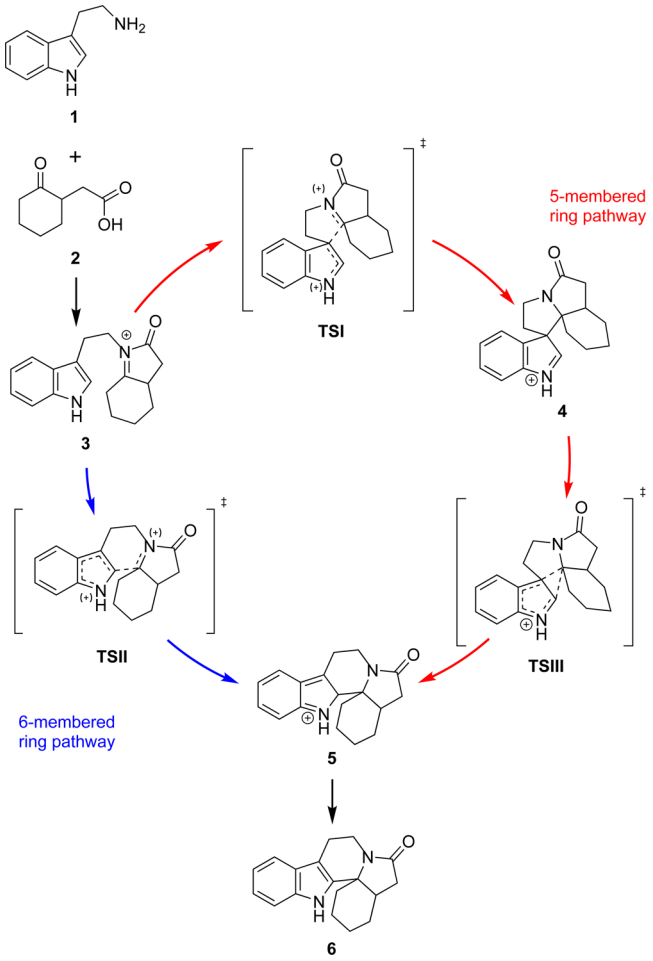

considerably higher in energy than the five- and six-membered ring formation TSs. They therefore concluded that the five-membered intermediate would not go on to form the six-membered intermediate via the ring expansion TS and would instead go back to the *N*-acyliminium ion and then on to the product via the six-membered TS and intermediate.

Several examples of asymmetric Pictet–Spengler reactions exist, including those that use chiral auxiliaries[16−18] and chiral catalysts,[19,20] such as 1,1′-bi-2-naphthol-derived (BINOL-derived) phosphoric acid catalysts.[1,21,22] BINOL-derived phosphoric acids have been used as catalysts in enantioselective versions of a wide range of reactions[23−35] and in several total syntheses.[36,37]

The asymmetric Pictet–Spengler reaction shown in Scheme 1 proceeds with 81% enantiomeric excess and 77% yield. Complexation with the 3,3′-bis(triphenylsilyl)-BINOL phosphoric acid catalyst **8** (Figure 1) changes the energies of the

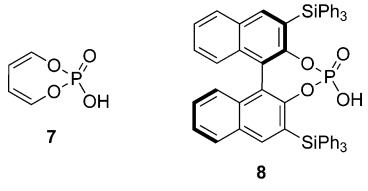

Figure 1. Model diene phosphoric acid catalyst (**7**) and 3,3′-bis(triphenylsilyl)-BINOL phosphoric acid catalyst (**8**).

eight possible diastereomers of **TSI**, **TSII**, and **TSIII**, hence leading to stereoinduction. However, it is unclear how the chiral catalyst catalyzes the reaction. A full understanding of the factors leading to selectivity would enable further development of this and related transformations.

2. RESULTS AND DISCUSSION

2.1. Five- or Six-Membered Ring? The relative energies of the different TSs and ground states (GSs) of the uncatalyzed reaction were found by use of density functional theory (DFT)[38] in Jaguar 2009[39] with the B3LYP density functional[40] and split-valence polarized 6-31G** basis set[41] with M06-2X single-point energy correction.[42,43] The stereochemistry of the structures in the pathways (Figure 2) and the Gibbs free energies of the transition structures in the uncatalyzed reaction to form **5** are shown in Table 1. These are quoted relative to the energy of **3** (*R*).

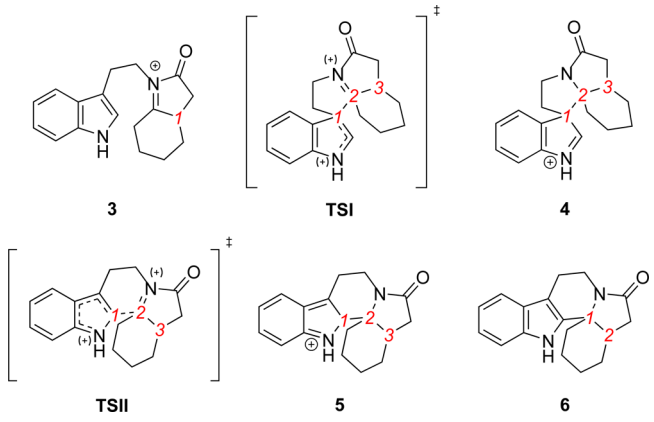

Figure 2. Numbering of stereogenic centers: for example, **TSII** (*RSR*) is *R* at position 1, *S* at position 2, and *R* at position 3.

The lowest energy TS is **TSII** (*SRR*) (Figure 3) [note that **TSII** (*SRR*) refers to the configuration of **TSII** that leads to **5** (*SRR*)]. The *SRR* and *RSR* diastereomers have chair conformations and are considerably lower in energy than the *RRR* and *SSR* TSs, which have twist boat conformations. The different diastereomers of **TSII** are forced to adopt these conformations by two five-membered rings in the structure (from the indole and from the lactam), which are approximately planar because they each have more than one sp^2 center.[44,45] **TSII** (*SRR*) is lower in energy than **TSII** (*RSR*) because of the 5,6 *cis*-fused bicyclic system formed by the lactam ring and the cyclohexane ring.[46]

All four **TSI** diastereomers are higher in energy than **TSII** (*SRR*), suggesting that the reaction goes via the six-membered ring pathway (Scheme 2). Despite extensive searching, no geometries of **TSIII** could be located. Kowalski et al.[15] and Maresh et al.[7] both found that, in the reaction of tryptamine and an aldehyde, the ring expansion TS was considerably higher in energy than the five- and six-membered ring-formation TSs. In the reaction studied by Holloway et al.,[1] the energy of **TSI** is prohibitively high for the formation of **4**, and hence formation of **TSIII** can be discounted.

TSII (*SRR*) is the only significantly populated transition state out of the different diastereomers of **TSI** and **TSII**, with a Boltzmann ratio of 0.999 763, suggesting that the uncatalysed reaction goes via the six-membered ring pathway through a geometry of **TSII** that leads to **5** (*SRR*). **5** (*SRR*) would lose a

DOI: 10.1021/jo5028134
J. Org. Chem. 2015, 80, 2634−2640

Table 1. Stereochemistry of Structures and Gibbs Free Energies of Transition Structures Relative to 3 (*R*) for the Uncatalyzed Reaction[a]

via five-membered ring								via six-membered ring					
3	→	**4**	→	**5**	→	**6**	$\Delta G^{\ddagger}_{TSI}$	**3**	→	**5**	→	**6**	$\Delta G^{\ddagger}_{TSII}$
R	→	*RRR*	→	*RRR*	→	*RR*	16.0	*R*	→	*RRR*	→	*RR*	16.3
R	→	*RSR*	→	*RSR*	→	*SR*	19.2	*R*	→	*RSR*	→	*SR*	11.8
R	→	*SRR*	→	*SRR*	→	*RR*	20.5	*R*	→	*SRR*	→	*RR*	5.4
R	→	*SSR*	→	*SSR*	→	*SR*	18.4	*R*	→	*SSR*	→	*SR*	19.3

[a]Structures are given in Figure 2. Energies were found by use of B3LYP/6-31G** with a M06-2X/6-31G** single-point energy correction. All energies are given in kilocalories per mole.

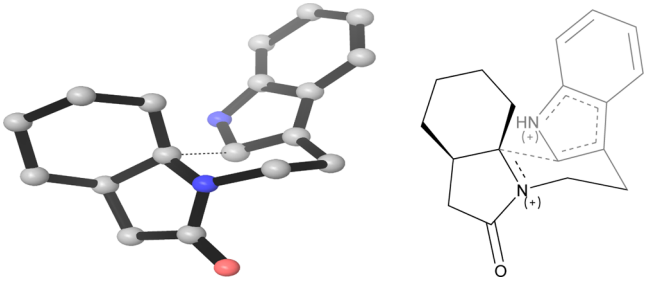

Figure 3. TSII (*SRR*) in the uncatalyzed reaction. Hydrogen atoms are omitted for clarity. Geometry B3LYP/6-31G**.

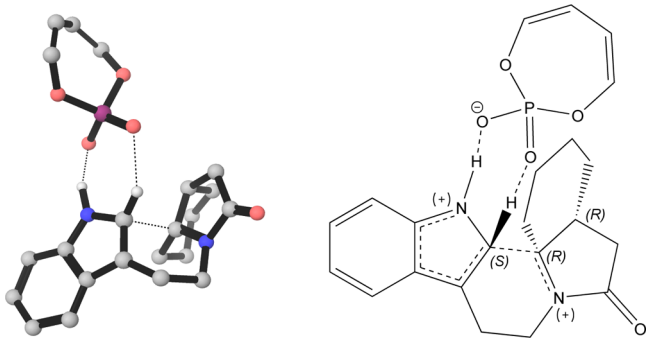

Figure 4. TSII (*SRR*) for the reaction catalyzed by model catalyst **7**. Hydrogen atoms are omitted for clarity. Geometry B3LYP/6-31G**.

proton to form **6** (*RR*), and the formation of this *cis*-fused product is consistent with the experimental evidence found by Holloway et al.[1]

2.2. Catalysis. The catalyzed reaction was first studied at the B3LYP/6-31G** level of theory with M06-2X single-point energy correction using a model diene phosphoric acid catalyst (**7**) (Figure 1).[47−49] The Gibbs free energies of the structures in the reaction catalyzed by **7** relative to **3**:**7** (*R*, *ab*) are shown in Table 2. The lowest energy TS remains **TSII** (*SRR*) (Figure 4), and the structures and relative energies of the different TS diastereomers are similar to those in the uncatalyzed reaction because the diene does not greatly affect the stereocenters of the substrate.

As with the uncatalyzed reaction, the Boltzmann ratios for the different diastereomers of **TSI** and **TSII** show that **TSII** (*SRR*) is the only significantly populated transition state. The Boltzmann ratio for **TSII** (*SRR*) is 0.999 945.

Two possible binding modes were found for **TSII** (*SRR*): *a* and *ab* (Figure 6). *ab* coordination is favored by 2.1 kcal·mol^{-1}. This bidentate binding holds the molecule in a fixed orientation relative to the catalyst, which could allow the full catalyst to differentiate between enantiomers. This interaction has previously been identified as playing a crucial role in a phosphoric acid-catalyzed reaction.[50]

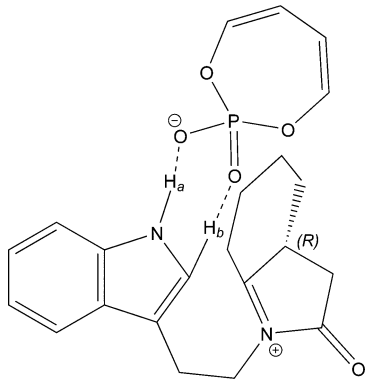

3:**7** (*R*, *ab*)

Figure 5. Complex of **3** (*R*) and **7**.

Calculations for the model catalyst **7** suggest that the stereochemistry of the reaction is not substantially affected by binding of the *N*-acyliminium ion to the catalyst phosphate group and that the catalyst binds to the transition state in a bidentate fashion, which could allow the full catalyst to

Table 2. Stereochemistry of Structures and Gibbs Free Energies of Transition Structures Relative to 3:7 (*R*, *ab*)[a] for the Reaction Catalyzed by Model Catalyst 7 with *ab* Coordination[b]

via five-membered ring								via six-membered ring					
3	→	**4**	→	**5**	→	**6**	$\Delta G^{\ddagger}_{TSII}$	**3**	→	**5**	→	**6**	$\Delta G^{\ddagger}_{TSII}$
R	→	*RRR*	→	*RRR*	→	*RR*	17.8	*R*	→	*RRR*	→	*RR*	23.1
R	→	*RSR*	→	*RSR*	→	*SR*	16.1	*R*	→	*RSR*	→	*SR*	14.2
R	→	*SRR*	→	*SRR*	→	*RR*	19.1	*R*	→	*SRR*	→	*RR*	6.5
R	→	*SSR*	→	*SSR*	→	*SR*	19.3	*R*	→	*SSR*	→	*SR*	23.0

[a]See Figure 5 for complex of **3** (*R*) and **7**. [b]Structures are given in Figure 2. Energies were found by use of B3LYP/6-31G** with a M06-2X/6-31G** single-point energy correction. All energies are given in kilocalories per mole.

DOI: 10.1021/jo5028134
J. Org. Chem. 2015, 80, 2634−2640

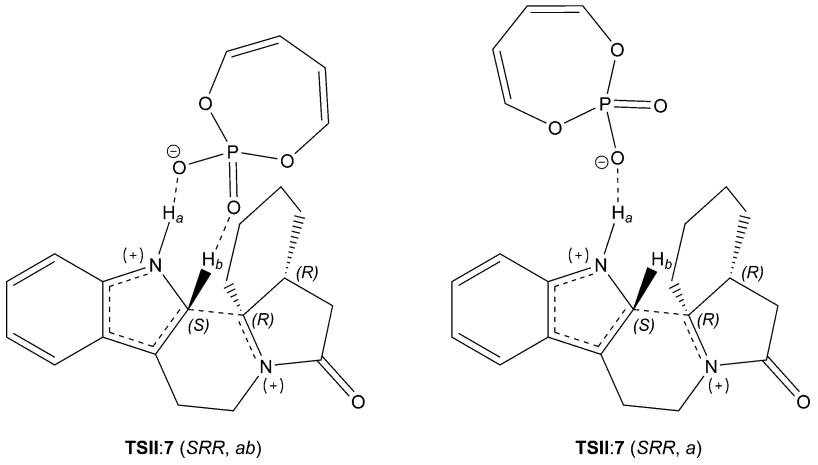

Figure 6. Two possible binding modes of **TSII** (*SRR*) and **7**.

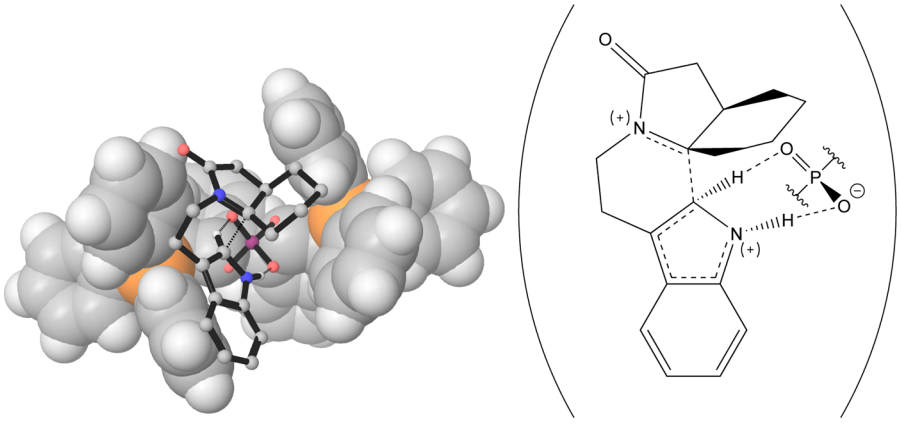

Figure 7. TSII (*SRR*) for the reaction catalyzed by **8**. Some hydrogen atoms are omitted for clarity. Geometry B3LYP/6-31G**.

Table 3. Stereochemistry of Structures and Gibbs Free Energies of Transition Structures Relative to 3:8 (*R, ab*)[a] for the Reaction Catalyzed by 8 with *ab* Coordination[b]

via five-membered ring								via six-membered ring					
3	→	**4**	→	**5**	→	**6**	$\Delta G^{\ddagger}_{TSI}$	**3**	→	**5**	→	**6**	$\Delta G^{\ddagger}_{TSII}$
R	→	*RRR*	→	*RRR*	→	*RR*	22.3	*R*	→	*RRR*	→	*RR*	24.1
S	→	*SSS*	→	*SSS*	→	*SS*	15.4	*S*	→	*SSS*	→	*SS*	18.8
R	→	*RSR*	→	*RSR*	→	*SR*	20.8	*R*	→	*RSR*	→	*SR*	18.4
S	→	*SRS*	→	*SRS*	→	*RS*	23.9	*S*	→	*SRS*	→	*RS*	19.9
R	→	*SRR*	→	*SRR*	→	*RR*	17.3	*R*	→	*SRR*	→	*RR*	9.2
S	→	*RSS*	→	*RSS*	→	*SS*	16.0	*S*	→	*RSS*	→	*SS*	12.2
R	→	*SSR*	→	*SSR*	→	*SR*	23.4	*R*	→	*SSR*	→	*SR*	25.0
S	→	*RRS*	→	*RRS*	→	*RS*	22.8	*S*	→	*RRS*	→	*RS*	30.0

[a]See Figure 8 for complex of **3** (*R*) and **8**. [b]Structures are shown in Figure 2. Energies were found by use of B3LYP/6-31G**:UFF ONIOM with a M06-2X/6-31G** single-point energy correction. All values are given in kilocalories per mole.

differentiate between different geometries of the transition states.

2.3. Enantioselectivity. To investigate whether the BINOL-derived phosphoric acid catalyst can confer selectivity between **TSII** (*SRR*) and **TSII** (*RSS*), which have identical energies in the absence of a catalyst, the full catalyst molecule must be considered. Hybrid quantum mechanics/molecular mechanics (QM/MM) calculations by the ONIOM[51] method in Gaussian03[52] were used to reduce computational time when the full catalyst structure was considered. DFT (B3LYP/6-31G**) was used for the high layer and MM[53] [universal force field (UFF)[54]] for the low layer, with M06-2X single-point energy correction subsequently applied to the whole structure. The use of ONIOM with B3LYP/6-31G** and UFF layers has been previously shown to give good results when BINOL-derived phosphoric acid catalysis was described.[55]

The substrate and phosphate group were included in the high layer and the rest of the catalyst in the low layer because the phosphate group provides a key binding interaction whereas the rest of the catalyst acts as steric bulk and can be adequately described by MM.

The lowest energy TS remains as **TSII** (*SRR*) (Figure 7) when the full catalyst structure is considered. Table 3 shows that all diastereomers of **TSII** coming from **3** (*S*) are lower in

DOI: 10.1021/jo5028134
J. Org. Chem. 2015, 80, 2634−2640

energy those coming from **3** (*R*), except for **TSII** (*SRS*), where the fused cyclohexane ring is in a boat conformation, whereas in **TSII** (*RSR*) it is in a chair conformation and therefore is lower in energy (Supporting Information).

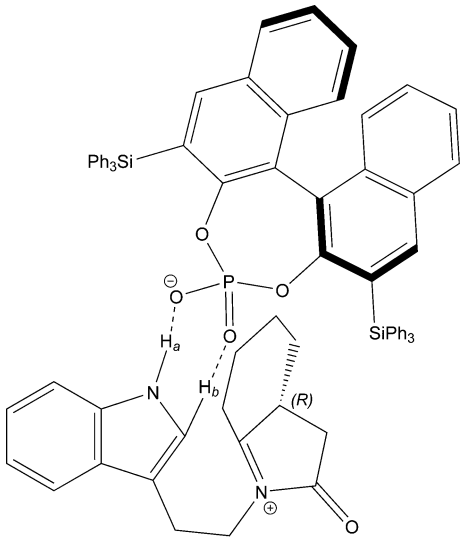

3:**8** (*R*, *ab*)

Figure 8. Complex of **3** (*R*) and **8**.

Reasons for the selectivity toward **6** (*RR*) originate from the unfavorable steric clash between the six-membered ring of the 5,6-bicyclic system and the large catalyst substituent in **TSII** (*RSS*) (Figure 9). The substrate adopts close to a flat conformation apart from this six-membered ring, which preferentially orientates itself toward the empty pocket of the chiral catalyst in **TSII** (*SRR*), leading to the observed enantioselectivity (Figure 9). These results are consistent with the findings from our study of aldehyde allylboration and allenylboration demonstrating the generality of this reaction model.[43,47]

All eight **TSI** diastereomers are again higher in energy than **TSII** (*SRR*) and the Boltzmann ratio for **TSII** (*SRR*) is 0.981, indicating that it is the major pathway.

If it is assumed that conversion from **5** to **6** is irreversible, this would lead to a diastereomeric ratio in the final products of 9.81×10^{-1} (*RR*):1.92×10^{-2} (*SS*):6.05×10^{-6} (*SR*):8.52×10^{-7} (*RS*), which agrees qualitatively with experimental results but slightly overestimates the enantiomeric excess (96% vs 81%).

Solvent effects were investigated by single-point energy calculations in Jaguar with M06-2X/6-31G** and the polarizable continuum model.[56] These energies were used to correct the gas-phase B3LYP/6-31G** calculations. The difference in Gibbs free energies between **TSII** (*SRR*) and **TSII** (*RSS*) in toluene was found to be 2.7 kcal·mol^{-1}, compared with 3.0 kcal·mol^{-1} in the gas phase. These results suggest that the solvent does not greatly affect the differences in energies between the TSs. Hence, it seems reasonable to use calculations performed in the gas phase to investigate this reaction.

Simón and Goodman[55] proposed a model for predicting the stereochemistry of a BINOL-phosphoric acid-catalyzed Hantzsch ester imine reduction that can also be applied to this system (Figure 9). The fused cyclohexane ring of **TSII** (*SRR*) avoids the triphenylsilyl group at the front of the catalyst by pointing into the empty space on the right, whereas in **TSII** (*RSS*) the ring points toward the triphenylsilyl group, leading to

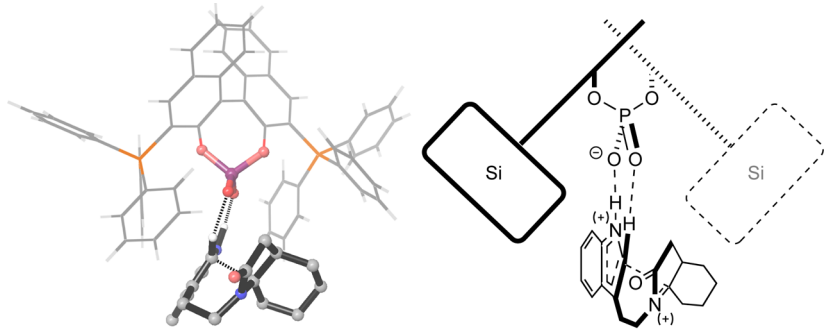

TSII (*SRR*) 0.0 kcal mol^{-1}

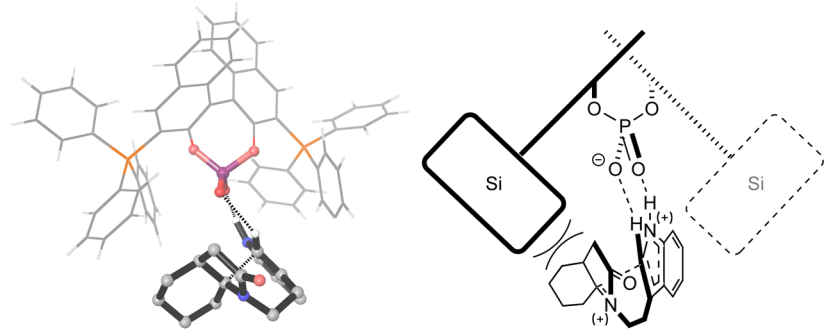

TSII (*RSS*) +3.0 kcal mol^{-1}

Figure 9. Comparison of **TSII** (*SRR*) and **TSII** (*RSS*) by use of the model proposed by Simón and Goodman.[55] Gibbs free energies are relative to **TSII** (*SRR*). Some hydrogen atoms are omitted for clarity. Geometry B3LYP/6-31G**:UFF ONIOM, energies B3LYP/6-31G**:UFF ONIOM with M06-2X/6-31G** single-point energy correction.

DOI: 10.1021/jo5028134
J. Org. Chem. 2015, 80, 2634−2640

steric clash and an increase in energy as the molecule twists to avoid the triphenylsilyl group, thus weakening the hydrogen bonding to the phosphate. This leads to a change in the P−O−H_b−C_2 dihedral angle from 23.5° to −54.4°, the H_a−O bond distance from 1.48 to 1.54 Å, and the H_b−O bond distance from 2.00 to 2.30 Å.

Consideration of the full catalyst structure suggests that **TSII** (*SRR*) is favored over **TSII** (*RSS*). **TSII** (*SRR*) leads to **6** (*RR*); hence the calculations are in agreement with the experimental results.

3. CONCLUSIONS

DFT and QM/MM hybrid calculations suggest that the phosphoric acid-catalyzed Pictet−Spengler reaction involves a highly ordered transition structure in which there is a hydrogen-bonding interaction from the catalyst to the NH proton of the indole. An additional stabilizing CH−O interaction lowers the energy of the transition structure and provides extra rigidity to the system. This activation mode successfully accounts for the sense and level of enantioselectivity observed experimentally. A qualitative guide to rationalizing the experimental results has been suggested (Figure 9). The model gives a clear mechanistic insight into this reaction and should serve to promote further development of synthetic methodology involving this mode of activation.

4. EXPERIMENTAL SECTION

Different conformations of the starting materials, intermediates, products, and TSs were found by a conformational search in MacroModel (version 9.6)[57] using an OPLS 2005 force field.[58] The mixed torsional/low mode sampling method was used,[59] which uses the Monte Carlo multiple minimum method[60] to explore the possible conformations of a molecule or complex. The conformers within 5.0 kcal·mol^{-1} of the minimum energy conformer were optimized by use of DFT or ONIOM.

Uncatalyzed reactions and the reactions catalyzed by model catalyst **7** were studied by DFT in Jaguar 2009[39] with the B3LYP density functional[40] and split-valence polarized 6-31G** basis set.[41] Structures were found by use of unconstrained optimizations with the default convergence criteria, medium grid density, and quick accuracy level. TSs were found by the standard transition-state search (STS) method.

Structures involving the full BINOL-derived phosphoric acid catalyst (**8**) were optimized by use of hybrid QM/MM calculations with the ONIOM method in Gaussian 03.[52] B3LYP/6-31G** was used for the high layer and universal force field (UFF)[54] for the low layer. The use of ONIOM with B3LYP/6-31G** and UFF layers has been previously shown to give good results when BINOL-derived phosphoric acid catalysis is described.[55]

Gas-phase energies were zero-point energy-corrected with a scale factor of 0.9.[61] Gibbs free energies were corrected[42] by use of Jaguar single-point energy calculations with the M06-2X density functional.[62]

To find the Gibbs free energies in solution, the Gibbs free energies of structures optimized in the gas phase were corrected with a single-point calculation by use of M06-2X/6-31G* and the polarizable continuum model with toluene (probe radius = 2.76 Å) in Jaguar.[39]

■ ASSOCIATED CONTENT

Supporting Information

Full Gaussian reference;[52] absolute energies including zero-point energy corrections, free energies, free energies including M06-2X energy corrections, number of imaginary frequencies for all stationary points, values of imaginary frequencies for all transition structures, and Cartesian coordinates for all compounds. This material is available free of charge via the Internet at http://pubs.acs.org.

■ AUTHOR INFORMATION

Corresponding Author

*E-mail jmg11@cam.ac.uk; phone +44 (0)1223 336434; fax +44 (0)1223 763076.

Notes

The authors declare no competing financial interest.

■ ACKNOWLEDGMENTS

We thank Girton College, Cambridge (research fellowship to M.N.G.), the EPSRC (studentship to M.N.G.), and Unilever for support.

■ REFERENCES

(1) Holloway, C. A.; Muratore, M. E.; Storer, R. I.; Dixon, D. J. *Org. Lett.* **2010**, *12*, 4720−4723.
(2) Holloway, C. A. Stereoselective construction of quaternary centres under Brønsted acid catalysis. Ph.D. thesis, University of Manchester, U.K., 2010.
(3) Pictet, A.; Spengler, T. *Ber. Dtsch. Chem. Ges.* **1911**, *44*, 2030−2036.
(4) Bailey, P. D.; Morgan, K. M. *Chem. Commun.* **1996**, *17*, 1479−1480.
(5) Xu, Y.-C.; Kohlman, D. T.; Liang, S. X.; Erikkson, C. *Org. Lett.* **1999**, *1*, 1599−1602.
(6) Pearson, W. H.; Lian, B. W. *Angew. Chem., Int. Ed.* **1998**, *37*, 1724−1726.
(7) Maresh, J. J.; Giddings, L.-A.; Friedrich, A.; Loris, E. A.; Panjikar, S.; Trout, B. L.; Stöckigt, J.; Peters, B.; O'Connor, S. E. *J. Am. Chem. Soc.* **2008**, *130*, 710−723.
(8) Luk, L. Y. P.; Bunn, S.; Liscombe, D. K.; Facchini, P. J.; Tanner, M. E. *Biochemistry* **2007**, *46*, 10153−10161.
(9) McQuillin, F. J.; Baird, S. *Alicyclic Chemistry*; Cambridge University Press: Cambridge, U.K., 1983.
(10) Sorrell, T. N. *Organic Chemistry*; University Science Books: Herndon, VA, 2006.
(11) Jackson, A. H.; Smith, P. *Chem. Commun.* **1967**, 264−266.
(12) Anslyn, E. V.; Dougherty, D. A. *Modern Physical Organic Chemistry*; University Science Books: Herndon, VA, 2006.
(13) Baldwin, J. E. *J. Chem. Soc., Chem. Commun.* **1976**, 734−736.
(14) Bailey, P. D.; Hollinshead, S. P.; McLay, N. R. *Tetrahedron Lett.* **1987**, *28*, 5177−5180.
(15) Kowalski, P.; Bojarski, A. J.; Mokrosz, J. L. *Tetrahedron* **1995**, *51*, 2737−2742.
(16) Li, J.; Wang, T.; Yu, P.; Peterson, A.; Weber, R.; Soerens, D.; Grubisha, D.; Bennett, D.; Cook, J. M. *J. Am. Chem. Soc.* **1999**, *121*, 6998−7010.
(17) Kawate, T.; Yamanaka, M.; Nakagawa, M. *Heterocycles* **1999**, *50*, 1033−1039.
(18) Lee, A. W.; Chan, W. H.; Lee, Y.-K. *Tetrahedron Lett.* **1991**, *32*, 6861−6864.
(19) Kawate, T.; Yamada, H.; Soe, T.; Nakagawa, M. *Tetrahedron: Asymmetry* **1996**, *7*, 1249−1252.
(20) Klausen, R. S.; Jacobsen, E. N. *Org. Lett.* **2009**, *11*, 887−890.
(21) Seayad, J.; Seayad, A. M.; List, B. *J. Am. Chem. Soc.* **2006**, *128*, 1086−1087.
(22) Wanner, M. J.; van der Haas, R. N. S.; de Cuba, K. R.; van Maarseveen, J. H.; Hiemstra, H. *Angew. Chem., Int. Ed.* **2007**, *46*, 7485−7487.
(23) Uraguchi, D.; Terada, M. *J. Am. Chem. Soc.* **2004**, *126*, 5356−5357.
(24) Yamanaka, M.; Itoh, J.; Fuchibe, K.; Akiyama, T. *J. Am. Chem. Soc.* **2007**, *129*, 6756−6764.
(25) Jain, P.; Wang, H.; Houk, K. N.; Antilla, J. C. *Angew. Chem.* **2012**, *124*, 1420−1423.
(26) Jain, P.; Antilla, J. C. *J. Am. Chem. Soc.* **2010**, *132*, 11884−11886.
(27) Reddy, L. R. *Chem. Commun.* **2012**, *48*, 9189−9191.

DOI: 10.1021/jo5028134
J. Org. Chem. 2015, 80, 2634−2640

(28) Kang, Q.; Zhao, Z.-A.; You, S.-L. *J. Am. Chem. Soc.* **2007**, *129*, 1484−1485.
(29) Jia, Y.-X.; Zhong, J.; Zhu, S.-F.; Zhang, C.-M.; Zhou, Q.-L. *Angew. Chem., Int. Ed.* **2007**, *46*, 5565−5567.
(30) Rueping, M.; Sugiono, E.; Azap, C. *Angew. Chem., Int. Ed.* **2006**, *45*, 2617−2619.
(31) Storer, R. I.; Carrera, D. E.; Ni, Y.; MacMillan, D. W. C. *J. Am. Chem. Soc.* **2006**, *128*, 84−86.
(32) Liu, H.; Cun, L.-F.; Mi, A.-Q.; Jiang, Y.-Z.; Gong, L.-Z. *Org. Lett.* **2006**, *8*, 6023−6026.
(33) Terada, M.; Machioka, K.; Sorimachi, K. *J. Am. Chem. Soc.* **2007**, *129*, 10336−10337.
(34) Pan, S. C.; Zhou, J.; List, B. *Angew. Chem., Int. Ed.* **2007**, *46*, 612−614.
(35) Jiang, J.; Yu, J.; Sun, X.-X.; Rao, Q.-Q.; Gong, L.-Z. *Angew. Chem., Int. Ed.* **2008**, *47*, 2458−2462.
(36) Wanner, M. J.; Boots, R. N. A.; Eradus, B.; de Gelder, R.; van Maarseveen, J. H.; Hiemstra, H. *Org. Lett.* **2009**, *11*, 2579−2581.
(37) Cheng, M.-N.; Wang, H.; Gong, L.-Z. *Org. Lett.* **2011**, *13*, 2418−2421.
(38) Hohenberg, P.; Kohn, W. *Phys. Rev.* **1964**, *136*, B864−B871.
(39) *Jaguar version 7.6*; Schrödinger LLC, New York, 2009.
(40) Becke, A. D. *Phys. Rev. A* **1988**, *38*, 3098−3100.
(41) Krishnan, R.; Binkley, J. S.; Seeger, R.; Pople, J. A. *J. Chem. Phys.* **1980**, *72*, 650−654.
(42) Simón, L.; Goodman, J. M. *Org. Biomol. Chem.* **2011**, *9*, 689−700.
(43) Grayson, M. N.; Goodman, J. M. *J. Am. Chem. Soc.* **2013**, *135*, 6142−6148.
(44) Chadwick, D.; Legon, A. C.; Millen, D. J. *J. Chem. Soc. Faraday Trans. 2* **1979**, *75*, 302−311.
(45) Saebø, S.; Cordell, F. R.; Boggs, J. E. *J. Mol. Struct.: THEOCHEM* **1983**, *104*, 221−232.
(46) Gordon, H. L.; Freeman, S.; Hudlicky, T. *Synlett* **2005**, *19*, 2911−2914.
(47) Grayson, M. N.; Pellegrinet, S. C.; Goodman, J. M. *J. Am. Chem. Soc.* **2012**, *134*, 2716−2722.
(48) Grayson, M. N.; Goodman, J. M. *J. Org. Chem.* **2013**, *78*, 8796−8801.
(49) Simón, L.; Goodman, J. M. *J. Org. Chem.* **2011**, *76*, 1775−1788.
(50) Maity, P.; Pemberton, R. P.; Tantillo, D. J.; Tambar, U. K. *J. Am. Chem. Soc.* **2013**, *135*, 16380−16383.
(51) Svensson, M.; Humbel, S.; Froese, R. D. J.; Matsubara, T.; Sieber, S.; Morokuma, K. *J. Phys. Chem.* **1996**, *100*, 19357−19363.
(52) Frisch, M. J. et al. *Gaussian 03, Revision C.02*; Gaussian, Inc., Wallingford, CT, 2004.
(53) Burkert, U.; Allinger, N. L. *Molecular Mechanics*; American Chemical Society: Washington, DC, 1982.
(54) Rappe, A. K.; Casewit, C. J.; Colwell, K. S.; Goddard, W. A.; Skiff, W. M. *J. Am. Chem. Soc.* **1992**, *114*, 10024−10035.
(55) Simón, L.; Goodman, J. M. *J. Am. Chem. Soc.* **2008**, *130*, 8741−8747.
(56) Mennucci, B.; Tomasi, J. *J. Chem. Phys.* **1997**, *106*, 5151.
(57) Mohamadi, F.; Richards, N. G. J.; Guida, W. C.; Liskamp, R.; Lipton, M.; Caufield, C.; Chang, G.; Hendrickson, T.; Still, W. C. *J. Comput. Chem.* **1990**, *11*, 440−467.
(58) Kaminski, G. A.; Friesner, R. A.; Tirado-Rives, J.; Jorgensen, W. L. *J. Phys. Chem. B* **2001**, *105*, 6474−6487.
(59) Kolossváry, I.; Guida, W. C. *J. Comput. Chem.* **1999**, *20*, 1671−1684.
(60) Chang, G.; Guida, W. C.; Still, W. C. *J. Am. Chem. Soc.* **1989**, *111*, 4379−4386.
(61) Grev, R. S.; Janssen, C. L.; Schaefer, H. F. *J. Chem. Phys.* **1991**, *95*, 5128.
(62) Becke, A. D. *J. Chem. Phys.* **1996**, *104*, 1040−1046.

DOI: 10.1021/jo5028134
J. Org. Chem. 2015, 80, 2634−2640